



HAL
open science

PSE-based sensitivity analysis of turbulent and supersonic single stream jet

Tobias Ansaldi, Christophe Airiau, Carlos Pérez Arroyo, Guillaume Puigt

► **To cite this version:**

Tobias Ansaldi, Christophe Airiau, Carlos Pérez Arroyo, Guillaume Puigt. PSE-based sensitivity analysis of turbulent and supersonic single stream jet. 22nd AIAA/CEAS Aeroacoustics Conference, May 2016, Lyon, France. pp.0, 10.2514/6.2016-3052 . hal-02079182

HAL Id: hal-02079182

<https://hal.science/hal-02079182v1>

Submitted on 25 Mar 2019

HAL is a multi-disciplinary open access archive for the deposit and dissemination of scientific research documents, whether they are published or not. The documents may come from teaching and research institutions in France or abroad, or from public or private research centers.

L'archive ouverte pluridisciplinaire **HAL**, est destinée au dépôt et à la diffusion de documents scientifiques de niveau recherche, publiés ou non, émanant des établissements d'enseignement et de recherche français ou étrangers, des laboratoires publics ou privés.





Open Archive Toulouse Archive Ouverte (OATAO)

OATAO is an open access repository that collects the work of Toulouse researchers and makes it freely available over the web where possible.

This is an author-deposited version published in: [http://oatao.univ-toulouse.fr/Eprints ID: 18308](http://oatao.univ-toulouse.fr/Eprints/18308)

To link to this article : DOI:10.2514/6.2016-3052

URL : <https://doi.org/10.2514/6.2016-3052>

To cite this version: Ansaldi, Tobias  and Airiau, Christophe  and Pérez Arroyo, Carlos and Puigt, Guillaume *PSE-based sensitivity analysis of turbulent and supersonic single stream jet.* (2016) In: 22nd AIAA/CEAS Aeroacoustics Conference, 30 May 2016 - 1 June 2016 (Lyon, France)

Any correspondence concerning this service should be sent to the repository administrator: staff-oatao@listes-diff.inp-toulouse.fr

PSE-based sensitivity analysis of turbulent and supersonic single stream jet

Tobias Ansaldi* and Christophe Airiau†

*Institut de Mécanique des Fluides de Toulouse, UMR 5502 CNRS/INPT-UPS,
Université de Toulouse, Allée du Professeur Camille Soula, F31400 Toulouse, France*

Carlos Pérez Arroyo‡ and Guillaume Puigt

CERFACS, Computational Fluid Dynamics, 42 avenue Coriolis, F31057 Toulouse CEDEX, France.

Reducing noise emission from jet is a major topics of aeroacoustics. Recently, it has been shown that the large coherent structures of a turbulent single-stream jet, which are parts of the noise generation mechanisms, can be interpreted as instability of the mean turbulent flow, especially in the region of the potential core. Reducing noise will be probably only achieved with some new control strategy on the underlying physics of the acoustic wave generation. The present work deals with the last investigations associated to the sensitivity analysis of the single and dual-stream jet instability to any local forcing. Sensitivity is a first step of any aeroacoustic or flow control approach and it is performed by the Parabolized Stability Equations and their adjoint counter part. Validation is first made on a simple semi-analytical supersonic jet. Then sensitivity functions to a source of momentum, mass or energy forcing are given in a supersonic single ($M = 1.15$) and dual-stream jets ($M_p = 0.89$ and $M_s = 1.20$). The base-flow is obtained from accurate Large Eddy Simulations and included some shock cells. Highest sensitivities are found inside the shear layer close to the external boundary of the potential core and close to the jet inlet, similar to the previous results found in incompressible single stream jet. The growth rate and wave number of the Kelvin-Helmholtz instability and the acoustic (pressure) perturbation are strongly influenced by the shock cell positions.

I. Introduction

The study of the sensitivity of the flow and of its disturbances to any external localized or global forcing, is crucial for a better understanding of the physics or aeroacoustic control in jets. It can be remembered that the role of coherent structures in the production of turbulent jet noise, especially for compressible flow, has been demonstrated by experimental, computational and theoretical results.¹⁻⁹ It is also concluded that these large-scale coherent structures are the instability waves of the jet. Several methods are explored to compute the turbulent mixing noise from supersonic jets. In this work assuming that the large-scale structures can be modelled as the flow field generated by the evolution of instability waves in a given turbulent jet, the mean flows are obtained by solving Large Eddy Simulations (LES). The growth rate and the streamwise wavenumber of a disturbance with a fixed frequency and azimuthal wavenumber are obtained by solving the non-local approach called Parabolized Stability Equations (PSE). The PSE equations are solved by a space marching procedure with a remarkable reduction of computational time if compared with other methods like RANS, LES or Direct Numerical Simulation (DNS).

A first sensitivity analysis of jet instabilities associated to compressible jets at low Mach number has been performed and validated recently by coupling the PSE and the Adjoint-PSE method.^{12,17} In parallel, Tissot et al.¹⁹ proposed, using some PSE-4D-Var approach to investigate the role of the critical layer of a

*PhD student, Marie Curie Fellow, tobias.ansaldi@imft.fr

†Professor, University of Toulouse, christophe.airiau@imft.fr

‡PhD student, Marie Curie Fellow

jet in the presence of non-linear wave interactions. Precisely, They are looking for an optimal forcing that might improve the match between wavepacket solutions and measurements.

The main objective of this work is to investigate flow sensitivities to any disturbance in order to define some advanced noise control strategies. To the best of our knowledge, the sensitivity analysis in the framework of Adjoint Parabolized Stability Equations (APSE) of supersonic or dual-stream jets in relation with aeroacoustic has never been done before.

Following previous works,¹⁷ an extension of the compressible laminar flow to turbulent and supersonic flow is made in this paper and reminded in section II. The supersonic flow is based on a semi-analytical formulation.⁸ The new implementation is validated and sensitivities are performed in section III. In section IV are found the sensitivity analysis for two different supersonic under-expanded jet configurations where the baseflow is determined by time-average of Large Eddy Simulation (LES) profiles. The first configuration is a supersonic under-expanded single jet and the second one is a dual stream jet where the secondary stream is under-expanded and supersonic and the primary one is subsonic. Finally, the most sensitive zones related to some local forcing in the conservation stability equations are identified and discussed.

II. PSE and Adjoint-PSE in jet stability and sensitivity analysis

The Parabolized Stability Equations (PSE)¹⁵ approach used in this work consists on solving a set of Partial Differential Equations (PDE) mostly parabolic in the streamwise direction. PSE approach is now well known and applied in various stability problems. Several advantages can be shed on light. Indeed, contrary to the Linear Stability Theory (LST) where local parallel flow is assumed, they take into account the small streamwise variations of the base-flow and of the disturbances directly in the formulation. Since PSE are mathematically PDE, it is simple to solve them by adding various boundary conditions and source terms. This leads to use them for receptivity and sensitivity analysis,¹⁴ in optimal flow control approaches¹³ and for weakly nonlinear stability studies.¹⁵

In the following, all the variables are made non-dimensional. The characteristic length is based on the nozzle diameter and the characteristic flow properties are chosen to be those of the flow on the axis at the nozzle exit.⁴ The current study considers the total flow field vector written in cylindrical coordinates $\tilde{\mathbf{q}}(x, r, \theta, t)$ as a superposition of the mean steady flow $\bar{\mathbf{q}}(x, r, \theta)$ and the perturbation $\mathbf{q}'(x, r, \theta, t)$:

$$\tilde{\mathbf{q}} = \bar{\mathbf{q}} + \mathbf{q}' \quad \text{or} \quad \begin{pmatrix} \tilde{u}_x \\ \tilde{u}_r \\ \tilde{u}_\theta \\ \tilde{\rho} \\ \tilde{p} \end{pmatrix} = \begin{pmatrix} \bar{u}_x \\ \bar{u}_r \\ \bar{u}_\theta \\ \bar{\rho} \\ \bar{p} \end{pmatrix} + \begin{pmatrix} u'_x \\ u'_r \\ u'_\theta \\ \rho' \\ p' \end{pmatrix}, \quad (1)$$

where the nomenclature is defined as follows: u_x is the axial velocity, u_r is the radial velocity, u_θ is the azimuthal velocity, ρ is the density and p is the pressure.

Any perturbation \mathbf{q}' is assumed to have a wave-like exponential term $\chi(x)\exp(i(m\theta - \omega t))$ and an amplitude function $\mathbf{q}(x, r)$ that varies slowly with x as:

$$\mathbf{q}' = \mathbf{q}(x, r) \chi(x) \exp(i(m\theta - \omega t)), \quad \text{with} \quad \chi(x) = \exp\left[i \int_{x_0}^x \alpha(\xi) d\xi\right], \quad (2)$$

where i stands for the square root of -1 , $\alpha(x)$ is the complex axial wavenumber, m is the fixed integer azimuthal wavenumber, ω is the fixed angular frequency of the disturbance, x_0 is the inlet of the computational domain and t is the time. The imaginary part, $\alpha_i(x)$, can be defined as a growth rate and $2\pi/\alpha_r(x)$ corresponds to a spatial wavelength.

The decomposition is introduced into the Linearized Euler Equations (LEE) and the PSE are derived using the assumption of small streamwise variations of α , of \mathbf{q} and of the based flow quantities:

$$L_{PSE} \mathbf{q} = \mathbf{0}, \quad \text{with} \quad L_{PSE} = i\alpha A_1 + imA_2 - i\omega A_3 + B + A_1 \frac{\partial}{\partial x} + A_0 \frac{\partial}{\partial r}, \quad (3)$$

where A_0 , A_1 , A_2 , A_3 , B are matrix operators defined by the mean-flow properties and they are described by Ansaldo and Airiau (2015).¹⁷ From equation (2) it can be noticed that the streamwise change of the disturbance can be described by the product of the amplitude function and of the exponential term. This

ambiguity must be resolved by the introduction of an additional equation, called normalization or closure relationship, which imposes that the growth of the disturbance is absorbed by the wave function part of the decomposition of $\chi(x)$, making sure that the shape function $\mathbf{q}(x, r)$ stays with a slow variation in x .¹⁵ We set:

$$N(\mathbf{q}, x) = \int_0^\infty \mathbf{q}^h \frac{\partial \mathbf{q}}{\partial x} r dr = 0, \quad (4)$$

where the superscript h denotes the transpose conjugate. Equations (3) and (4) are solved using a streamwise marching solution starting from the initial condition at $x = x_0$ which is the solution of the local approach (LST). A compressible PSE solver designed by Leon and Brazier² has been used to get perturbation growth rate, wave number and shape function of the perturbation field.

As an initial step to further new noise control strategie research, the adjoint of PSE has been written specifically to investigate flow sensitivities to any disturbances of non-viscous jets. Sensitivity is mathematically equivalent to a gradient of any functional or quadratic integral.¹¹ This functional called E is closely related to the physical energy associated to the perturbed velocity, temperature and pressure and is defined as follows,

$$E = \int_\Omega \mathbf{q}^h M \mathbf{q}' r dr,$$

where M is a definite positive matrix, set here to identity and Ω refers to the computational domain.

A small local source forcing, $\hat{\mathbf{f}}(x, r)$, is applied as source term of the PSE. The sensitivity $S_{\hat{f}_k}$ with $k = 1, \dots, 5$ is therefore the gradient of E with respect to any component of the vector $\hat{\mathbf{f}}$, noted as \hat{f}_k :

$$S_{\hat{f}_k} = \nabla E_{\hat{f}_k}(\hat{f}_k = 0) = \left. \frac{\partial E}{\partial \hat{f}_k} \right|_{\hat{f}_k=0} \quad (5)$$

This relationship can be as well written in term of the variation as:

$$\delta E_{\hat{f}_k} = E(\hat{f}_k) - E(0) = \int_\Omega S_{\hat{f}_k} \delta \hat{f}_k d\Omega. \quad (6)$$

Here in the linear theory framework the small forcing is set by is own variation as $\delta \hat{f}_k = \hat{f}_k$, since the initial forcing is null. Depending on the value of k the forcing is acting respectively in the continuity, radial, azimuthal and axial momentum and in the energy equation.

An Adjoint-Lagrangian approach¹² is introduced to determine the sensitivity coefficients:

$$\mathcal{L}(\mathbf{q}, \hat{\mathbf{f}}, \alpha, \hat{\mathbf{q}}^*, n^*) = E - \int_\Omega \hat{\mathbf{q}}^{*h} (\chi L_{PSE} \mathbf{q} - \hat{\mathbf{f}}) d\Omega - \int_{x_0}^{x_f} \bar{n}^* \int_0^\infty \mathbf{q}^h \frac{\partial \mathbf{q}}{\partial x} r dr dx + c.c., \quad (7)$$

where the complex vector $\hat{\mathbf{q}}^*(x, r)$ and the complex function n^* are the Lagrange multipliers for the problem and they are respectively the dual variables of $\chi \mathbf{q}$ and α . Finally c.c. denotes the complex conjugate. This new real functional takes directly into account of the PSE equations and the related closing equation. There is no need to include in equation 7 the boundary and initial condition of the stability equations because they are always kept constant.

The different directional derivatives must vanish with the exception of those relative to the sensitivity term $S_{\hat{f}_k}$.¹⁷ Imposing this constraint and using the definitions of Eq. 5 and Eq. 6 the sensitivity function is the real part of an adjoint function:

$$S_{\hat{f}_k} = Re(\hat{q}_k^*) \quad (8)$$

The Lagrange multiplier $\hat{\mathbf{q}}^*$ is solution of the adjoint PSE equations which are similar to the PSE formulation but with a right-hand-side term:

$$L_{PSE}^* \hat{\mathbf{q}}^* = \frac{1}{\chi_f} \left[(n^* - \bar{n}^*) \frac{\partial \mathbf{q}}{\partial x} + \left(\frac{\partial n^*}{\partial x} + \chi \bar{\chi} \right) \mathbf{q} \right], \quad (9)$$

with

$$L_{PSE}^* = -\frac{1}{r} A_0^h + A^h + B^h - \frac{\partial A_1^h}{\partial x} - \frac{\partial A_0^h}{\partial r} - A_1^h \frac{\partial}{\partial x} - A_0^h \frac{\partial}{\partial r}.$$

For adjoint PSE, an additional closure relation is also found (Eq. 10) from the gradient of \mathcal{L} with respect to α :

$$\int_0^\infty (\chi \mathbf{q})^h \chi \mathbf{q} r dr + \int_0^\infty \left(\chi_f \frac{\partial (\mathbf{q}^{*h} A_1 \mathbf{q})}{\partial x} \right) r dr + c.c. = 0 \quad (10)$$

Boundary and terminal conditions of the adjoint state are obtained after some calculations and integration by part, as explained in details in Ansaldi and Airiau.¹⁷

Similar to the direct PSE, the full adjoint PSE system (9, 10 and boundary and terminal conditions) is solved using an iterative Newton-Raphson method. The adjoint PSE are discretized with a second order finite difference scheme in the streamwise direction and a sixth order compact difference scheme in the radial direction. An upwind marching procedure from the final x location x_f towards x_0 . The adjoint PSE has been validated in the case of subsonic single stream jets excited with a number of different external (source) forcing.¹⁷

In this paper the validation and analysis on different supersonic base-flow is provided. In addition, following a similar approach, adjoint PSE have been extended to study sensitivity of any parameter as for instance the frequency wave¹⁸.

III. Supersonic semi-analytical jet

The base-flow refers to a semi-empirical supersonic experimentation introduced by Tam et al (1982)¹ and often used in literature^{2,8,10} for stability studies. In this work, the computations of this base-flow are performed for a perfectly expanded jet at Mach number $M = 2.1$. As depicted by Tam et al,¹ the flow is divided into three regions as following:

1. Region I (or core region): $0 < x < x_t$

$$\bar{u}_x = \begin{cases} 1 & r < h \\ \exp \left[-\ln 2 \left(\frac{r - h(x)}{b(x)} \right)^2 \right] & r \geq h \end{cases} \quad (11)$$

2. Region II (or transitional region): $x_t \leq x < x_d$

$$\bar{u}_x = \begin{cases} u_c(x) & r < h \\ u_c(x) \exp \left[-\ln 2 \left(\frac{r - h(x)}{b(x)} \right)^2 \right] & r \geq h \end{cases} \quad (12)$$

3. Region III (or fully developed region): $x \geq x_d$

$$\bar{u}_x = u_c(x) \exp \left[-\ln(2) \left(\frac{r}{b(x)} \right)^2 \right] \quad (13)$$

Here, $h(x)$ is the radius of the uniform core and $b(x)$ is the distance from the half velocity location to the edge of the core. u_c is the velocity centerline. The function b is determined by a cubic spline from the experimental results of McLaughlin (1980).⁵ From McLaughlin (1980) work it is also found that the core region extends up to five diameters $x_t = 5$, and the fully developed region starts at eight diameters from the end of the nozzle $x_d = 8$. The value of h in the core region and u_c in the fully developed region are obtained imposing the conservation of axial momentum flow. In region II h and b are determined by a cubic interpolation. The coefficients of the cubic polynomial are chosen such that h and u_c and their first derivatives in x are continuous. The normalized density distribution $\bar{\rho}$ is obtained by solving Crocco-Busemann equations:

$$\begin{aligned} \bar{\rho} &= [-C_1 \bar{u}_x^2 + C_3 \bar{u}_x + C_2] \\ C_1 &= \frac{\gamma - 1}{2} M^2, \quad C_2 = \frac{T_a}{T_r} \left(1 + \frac{\gamma - 1}{2} M^2 \right) \\ C_3 &= C_1 - C_2 + 1. \end{aligned} \quad (14)$$

Where M is the Mach jet number ($M = 2.1$), T_a the plenum temperature and T_b the ambient temperature, in this paper $T_a = T_b$. The validity of the Crocco-Busemann law in jet plume has been checked computationally in the past.²³ In summary, for given Mach number, plenum and ambient temperatures, the density profile at a given axial station is uniquely dependent on the parameter b , the mixing layer half width.

Finally, the radial velocity \bar{u}_r is obtained by integrating the continuity equation along the radial direction.

Figure 1 shows the computed axial velocity. The edge of the potential core and of the shear layer can be clearly identified by the two dash-dot lines.

This base-flow profiles have been validated with the results from Yen and Messersmith⁸ and Balakumar.¹⁰ First the PSE equations are solved in order to determine the evolution of the instability waves inside the jet. The results are presented only for a Strouhal number $St = 0.4^8$ and for an axisymmetric perturbation ($m = 0$).

The adjoint PSE have been validated by solving directly computing the variation given in equation 6. The PSE equations (Eqs. 3-4) are therefore solved with and without a small amplitude forcing and the difference of the energy function is calculated at each streamwise location. The small variations are then compared with the integral term in Eq. 6 obtained by solving the adjoint PSE equations (Eqs.9-10). Several forcings with Gaussian distribution acting as a source term in one of the conservation equation have been tested in different regions of the base-flow. Because of the arbitrariness of this forcing, we keep the same forcing functions used to validate the subsonic jet.¹⁷ The small variation of the quantity E are shown in Fig. 2. They are determined from both approaches with a very good agreement. The extension of the sensitivity analysis to supersonic flow is therefore validated.

The normalized sensitivity coefficients with respect to conservation equation forcing are shown in Fig. 3. They are strongly dependent on the spatial coordinates x and r .

As expected, the sensitivity coefficients grow at the positions in the streamwise direction closer to the exit nozzle at x_0 . The maximum is reached close to the potential core in the shear layer of the jet in the range $x \in [0.45, 0.55]$ approximately. These conclusions are very similar to the ones found in the laminar subsonic jet. The results are well correlated with the location of the sound generation mechanism as seen in previous works.^{1,2}

IV. Supersonic under-expanded single and dual-stream jet

This section shows how stability analysis is applied to a turbulent supersonic under-expanded single and dual-stream jet. The main characteristic of under-expanded jets is the formation of a system of shock-cells at the exit of the nozzle that allows the jet to progressively expand to ambient conditions. This system is formed by a series of expansion and compression waves that bounce inside the potential core of the jet. The LES simulations have been carried out with the Finite Volume multi-block structured solver *elsA* (Onera's software²¹) and performed by the CERFACS.

IV.A. Turbulent single jet

The jet is under-expanded and at a perfectly expanded Mach number $M = 1.15$. Its Reynolds number is $Re = 1 \times 10^6$. This configuration has been tested experimentally by André.²⁰ The shock-cells manifested in the core of the flow, as seen in Fig. 4, interact with the instabilities around the potential core producing an intense noise as explained in Ray (2007).¹⁶

Pressure perturbations are propagated to the farfield by means of the Ffowcs Williams and Hawkings (FW-H)²⁴ analogy using the data on a topological surface located at $r/D = 3$. The results are shown in Fig. 5 (a) at different angles and compared with the experimental data of André.²⁰

The Sound Pressure Level (SPL) is in good agreement up to the mesh cut-off Strouhal. The Overall Sound Pressure Level (OASPL) is computed and compared with the experimental data in Fig. 5 (b). The simulation, being able to capture the main noise contributions of an under-expanded single jet, is a perfect base-flow to compute the stability and sensibility analysis.

From the LES data, temporal and azimuthal means have been done in order to produce the steady base-flow (Fig.4) on which the stability and sensitivity analyses are performed.

The stability results presented here refer to the axisymmetric instabilities with $m = 0$. The PSE computation has been initialized at the streamwise position $x = x_0$ and for a Strouhal number of $St = 0.890$ using Linear Stability Theory (LST) eigenmode.

Figure 6 shows the spatial distribution of the pressure perturbation p' at the nondimensional time $t = n/St$, where n is an integer number. The perturbation increases in the unstable regions of the flow ($Im(\alpha(x)) < 0$) and are damped down when the flow becomes stable. The spatial wavelength $\lambda = 2\pi/Re(\alpha)$ can also be guessed in the figure.

The influence of the frequency or Strouhal variations has to be study since the André's experimental spectrum (Fig 5) exhibits two screech noise frequencies.²⁰ The real and imaginary part of α are plotted on Fig. 7. The frequency dependence on the real wave number is obvious, and the shock cells locations are visible in the range of $x = 2$ to $x = 8$. It is natural since the stability properties are very sensitive to any mean flow variations. The variation of the frequency on the growth rate $Im(\alpha)$ are quite important close to the nozzle exit. Then, it seems that the growth rate is governed by the shock cells and not by the frequency. Downstream, when shock cells are weaker, the growth rate tends to be frequency independent (in the range of study).

Figure 8 provides the nondimensional sensitivity functions by forcing successively to every conservation equation and is expressed as a function of the adjoint state. It is equivalent to a local (Dirac) forcing. The maximum amplitude are weaker compared to the previous supersonic test case. The location of this maximum is strongly dependent on the streamwise coordinates and the highest sensitivity is closed to the nozzle exit.

The density and energy forcing are quite equivalent, similarly to the other subsonic and supersonic cases. For all the four different forcing the sensitivity is localized inside the shear layer and quickly decay along the streamwise direction. This results suggest that a flow control mechanism should be applied close to the exit nozzle, definitely before the end of the potential core, and in the shear layer region in order to obtain the highest response of the flow.

IV.B. Turbulent dual-stream jet

The case of study is a co-axial jet where the primary flow is cold and subsonic with an exit Mach number of $M_p = 0.89$ ($CNPR = 1.675$) and the secondary stream is operated at supersonic under-expanded conditions with a perfectly exit Mach number of $M_s = 1.20$ ($FNPR = 2.45$). Here, CNPR and FNPR stand for Core and Fan Nozzle to Pressure Ratio respectively. The jets are established from two concentric convergent nozzles with primary and secondary diameters of $D_p = 23.4mm$ and $D_s = 55.0mm$ respectively. The thicknesses of the nozzles at the exit are of $0.5mm$. The Reynolds numbers based on the jet exit diameters are $Re_p = 0.57 \times 10^6$ and $Re_s = 1.66 \times 10^6$. The lengths are non-dimensionalized by the internal diameter D_p . As in the previous case a temporal and azimuthal integral average have been done in order to produce the steady base-flow on which the stability analysis is performed and the PSE computation is initialized by a LST analysis. In the configuration of $St = 1.0$ two very distinct unstable modes are observed in the stability spectrum, Fig. 9. These two modes are the hydrodynamic Kelvin-Helmholtz modes (referred to as "KH modes") of the two mixing layer, KH_1 and KH_2 referring respectively to the inner and outer mixing regions.

The local growth of the KH_2 mode is larger than its related to KH_1 mode, which suggest a local dominance of the instability wave developing in the secondary jet. This first results is in according to the location of the production of noise found in.²² Clearly, this first trend found by the local stability theory has to be confirmed by the PSE non local approach to show the axial evolution of the disturbance. The pressure perturbation associated to the secondary modes KH_2 obtained by solving the PSE equations are shown in fig 10. The instability, as expected, grows in the secondary shear layer around the radial value $r/D_p = 1$ and slowly decays when the flow becomes stable.

Results for sensitivity analysis at this configuration are shown in fig 11 and 12. The sensitivity is solved for the both unstable modes, KH_1 and KH_2 . For both cases the sensitivity is spread along the two shear layers and goes to zero for greater values of r . The first important result is that the sensitivity is greater in the shear layer related to the unstable modes which initializes the PSE, but the secondary flow has the highest value for any forcing acting in the system. This result emphasize the role of the secondary jet in this configuration. However, we can clearly observe two distinct "zones" related to the primary and secondary shear layers. In the dual stream jet, and as it was found in the single stream jet, the density and energy sensitivity seems to exhibit a similar response along r . We still have a strong dependency in the r -direction and the local peak of these sensitivities are located at the primary and secondary shear layer radius. The maximum of amplitude are higher compared to the single jet case, suggesting a stronger response to the flow to external forcing.

V. Conclusion

In the present study the sensitivity analysis based on adjoint PSE of supersonic single-stream jet flow has been validated. The sensitivity with respect to underexpanded supersonic single and dual-stream jets has been considered. First configuration outlines a localized region where the response of the flow to external forcing is higher. This region has been identified close to the exit nozzle into the shear-layer in the external boundary of the potential core of the jet. The second configuration presents two unstable Kelvin-Helmholtz modes one for each shear-layer. The PSE and Adjoint-PSE computations show the central role of the secondary shear-layer, where the flow is more unstable and the sensitivity is higher. The local peaks of the sensitivity are located at the primary and secondary shear-layer radius highlighting the results of the single-stream jet case. However, to implement a new noise control strategy, for both cases, the strong dependence of the sensitivity to the spatial coordinates of the system suggest a very careful analysis of the interaction flow/actuator. This results have been obtained for both stability and sensitivity analysis, thanks to accurate LES computations from CERFACS.

Additional post-processing will be considered in further work, focus our attention on the physical explanation of the highest sensitivity location, exploiting the different locations of the critical layer, the inflection point, the shock-cell positions and the stability property (growth rate, wavenumber etc.).

Acknowledgments

This work has been supported by the European Community as part of the FP7-PEOPLE-2012-ITN AeroTraNet 2. We would like to thank J.P. Brazier and O. Léon from ONERA Toulouse for having provided the PSE code 'Pasteq'. This work was performed using HPC resources from CALMIP (grant 2014-24).

References

- ¹Tam, C. K. W. & Burton, D. E., *Sound generated by instability waves of supersonic flows. Part 2. Axisymmetric jets.*, J. Fluid. Mech. Vol. 138, pp. 273-295, 1982.
- ²Léon, O. & Brazier, J-P. *Application of Linear Parabolized Stability Equations to a Subsonic Coaxial Jet.* AIAA/CEAS, 32nd Aeroacoustics Conference, 2011-2839, 2011.
- ³Ray, P. K., Lawrence, C., Cheung, C. & Lele, S. K. *On the growth and propagation of linear instability waves in compressible turbulent jets.* Phys. Fluids Vol. 21, 2009.
- ⁴Piot, E., Casalis, G., Muller, F. & Bailly, C. *Investigation of the PSE approach for subsonic and supersonic hot jets.* Detailed comparison with LES and Linearized Euler Equations results. Aeroacoustic volume 5. 4, 361-393, 2006.
- ⁵McLaughlin, D. K., Seiner, J. M. and Liu, H. *On the noise generated by large scale instabilities in supersonic jets.* AIAA 80-0964, 1980.
- ⁶Yen, C. C. & Messersmith, N. L. *Application of Parabolized Stability Equations To the Prediction of jet Instabilities.* AIAA 98-16227, 1998.
- ⁷Ladeinde, F., Alabi, K., Colonius, T., Gudmundsson, K., Schlinker, R., and Reba, R., *An integrated RANS-PSE-wave packet tool for the prediction of subsonic and supersonic jet noise.* AIAA Paper 20104021, 2010.
- ⁸Yen, C. C. & Messersmith, N. L. *The use of Compressible Parabolized Stability Equations for Prediction of jet Instabilities and Noise.* AIAA 99-1859, 1999.
- ⁹Tam, C. K. W. *Directional acoustic radiation from a supersonic jet generated by shear layer instability.* J. Fluid Mech. 46 (4), 757-768, 1971.
- ¹⁰Balakumar, P. *Prediction of supersonic jet noise.* AIAA 98-1057, 1998.
- ¹¹Pralits J., Airiau C., Hanifi A. and Henningson D.S., *Sensitivity analysis using adjoint parabolized stability equations for compressible flows,* Flow, Turbulence and Combustion,
- ¹²Walther, S., Airiau, C. & Bottaro, A. *Optimal control of Tollmien-Schlichting waves in a developing boundary layer.* Phys. Fluids Vol. 13, 2001.
- ¹³Airiau, C. and Bottaro, A. and Walther, S. and Legendre, D. *A Methodology for Optimal Laminar Flow Control: Application to the Damping of Tollmien-Schlichting Waves in a Boundary Layer.* Phys. Fluids, vol. 15, (5), 1131-1145, 2003.
- ¹⁴Airiau C., Walther S. and Bottaro A., *Boundary layer sensitivity and receptivity,* C.R. Mécanique, vol. 330, 259265, 2002.
- ¹⁵Herbert, T. *Parabolized Stability Equations,* Annual Rev. Fluid. Mech. vol. 29, pp. 245-83, 1997.
- ¹⁶Ray, P.K and Lele, S., *Sound generated by instability wave/shock-cell interaction in supersonic jets.* J. Fluid Mechanics, Vol. 587, pp. 173215, 2007.
- ¹⁷Ansaldi, T. and Airiau, C., *Sensitivity analysis for subsonic jet using adjoint of non local stability equations* , AIAA Paper 2015-2219, 2015.
- ¹⁸Ansaldi, T., Granados Ortiz, F.-G., Airiau, C., Lai, C.-H., *Sensitivity and Uncertainty Quantification for jet stability analysis.* Congrès Français de Mécanique 74031 Lyon, 2015.
- ¹⁹Tissot, G., Zang, M., Lajús Jr., F.C., Cavalieri, A.V.G., Jordan, P and Colonius, T., *Sensitivity of wavepackets in jets to non-linear effects: the role of the critical layer.* AIAA-2218, 2015.

²⁰André, B., Castelain, T., and Bailly, C., *Broadband Shock-Associated Noise in Screeching and Non-Screeching Underexpanded Supersonic Jets*. AIAA J. Vol 51 (3), 665-673, 2013.

²¹Cambier, L., Heib, S., and Plot, S., *the Onera elsA CFD software: input from research and feedback from industry*. Mechanics and Industry, Vol 14 (3), pp. 159-174, 2013

²²Pérez, C., Puigt, G., Airiau, C. and Boussuge, J. F., *Large Eddy Simulation of Shock-Cell Noise From a Dual Stream Jet*. AIAA 2016.

²³Dahl, M. D., *The Aeroacoustics of Supersonic Coaxial Jets*. Ph. D. thesis, The Pennsylvania State University, 1994.

²⁴Ffowks Williams, J. E., and Hawkins, D. L., *Sound generation by turbulence and surfaces in arbitrary motion*. Philosophical Transactions of the Royal Society of London. Series A, Mathematical and Physical Sciences, 264, 321-342, 1969.

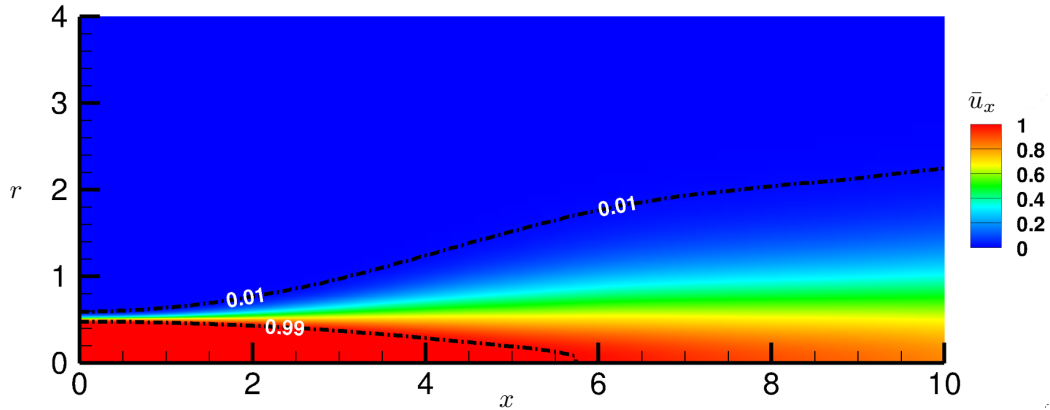


Figure 1. Spatial distribution of the mean axial velocity $M=2.1$. In dash-dot lines we have respectively the potential core and the boundary of the shear layer.

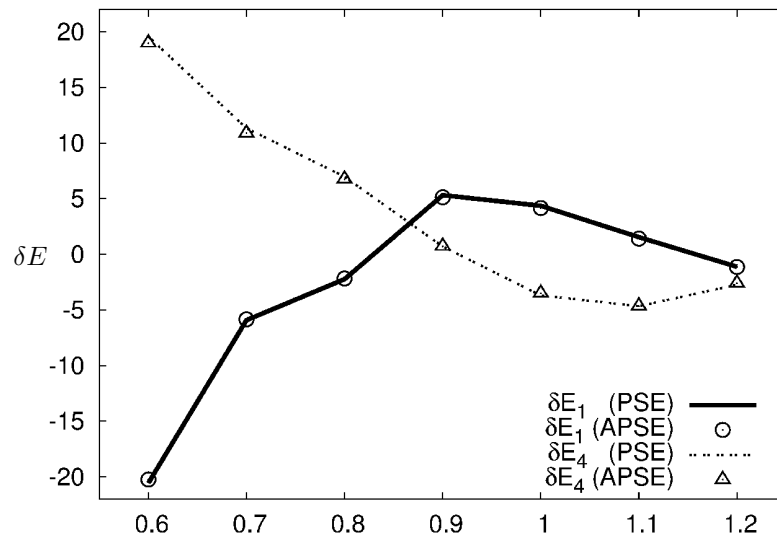


Figure 2. Comparison between results from PSE equations (lines) and from adjoint PSE equations (symbols) is made for the test case $M = 2.1$.

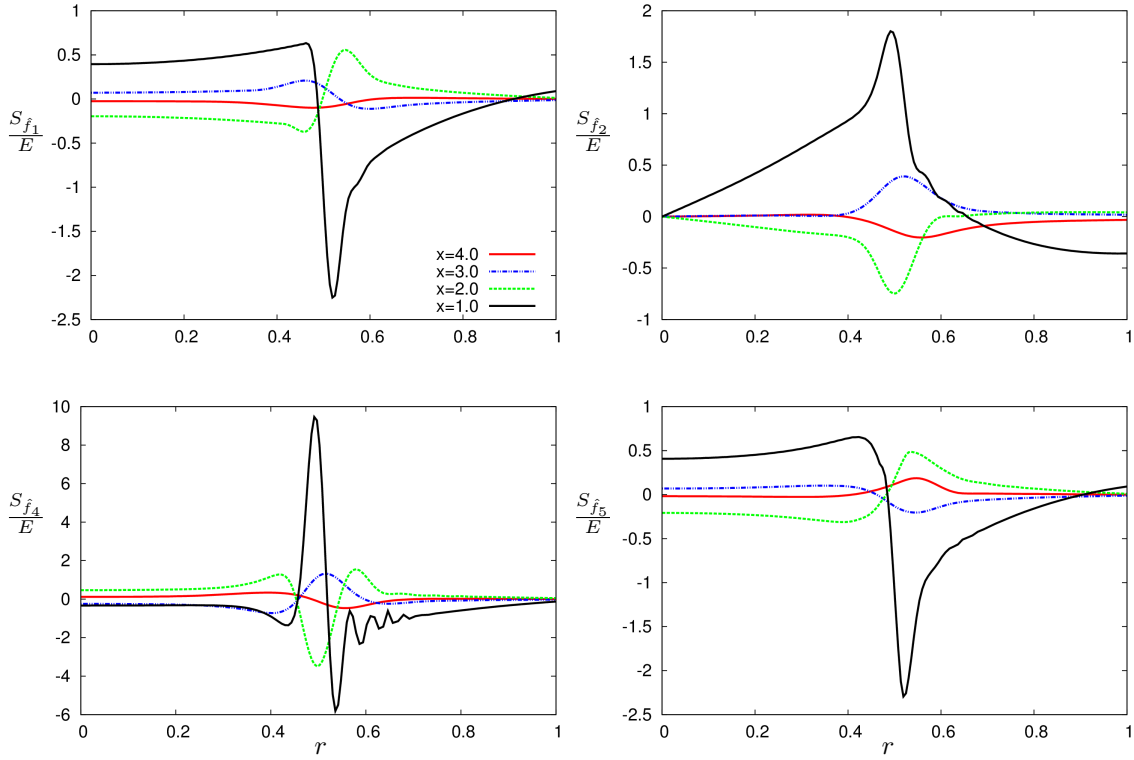


Figure 3. Sensitivity of the semi-analytical supersonic jet. From top the bottom we have respectively, the gradient of E with respect to the forcing acting in the continuity, r -momentum, x -momentum and energy equation at different fixed position in the stream-wise direction ($x = 4.0, 2.0, 1.0, 0.5$).

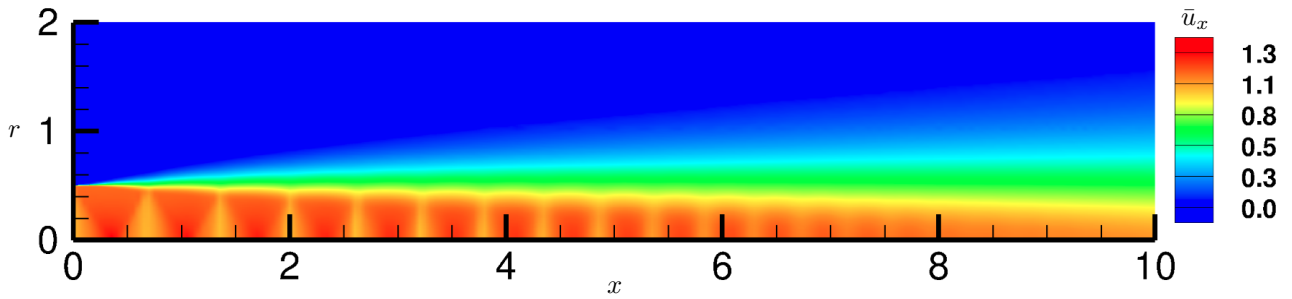


Figure 4. Spatial distribution of the mean axial velocity computed by LES. We can clearly observe the shock-cell distributed along the streamwise direction in the core of the jet.

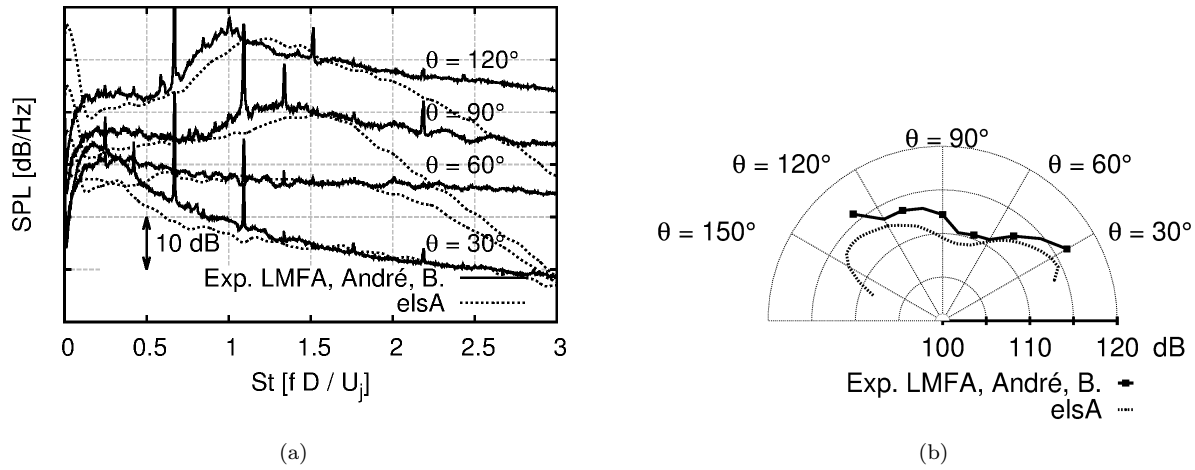


Figure 5. Acoustic spectrum in the farfield (50 diameters) for a $M_j = 1.15$ under-expanded jet. θ is measured with respect to the jet axis, (a) SPL, (b) OASPL.

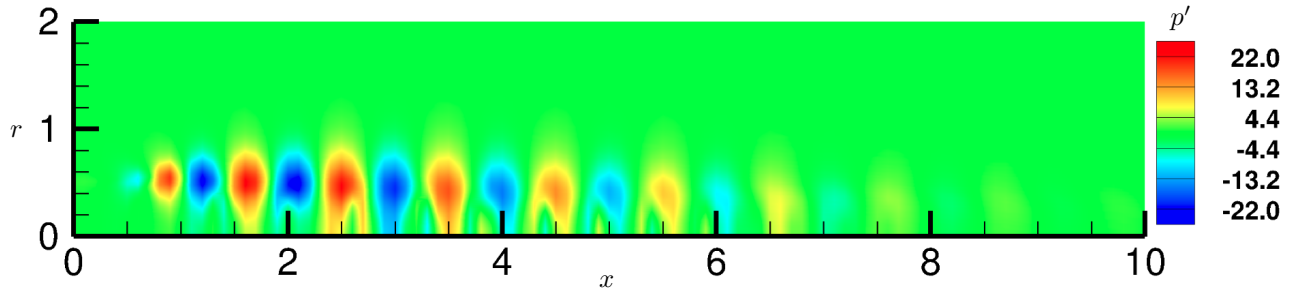


Figure 6. Spatial distribution of the perturbation p' for the Strouhal number $St = 0.89$, the pressure growth in the unstable regions of the jet and fall-down for high values of the streamwise coordinates where the flow is stable.

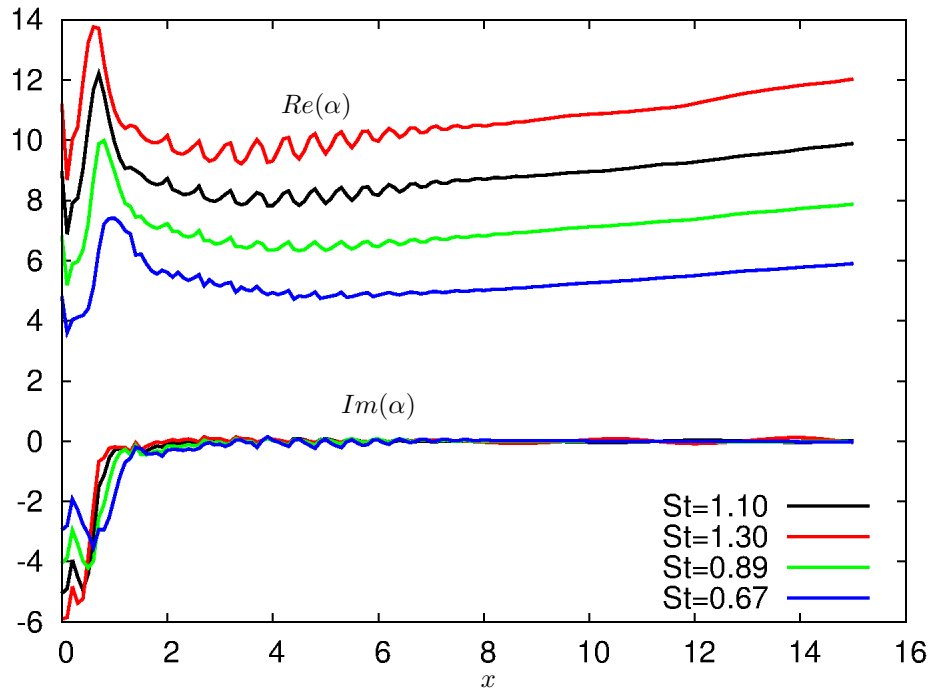


Figure 7. Axial distribution of the streamwise wave-number α for different values of the Strouhal number, respectively 1.10, 1.30, 0.89, 0.67.

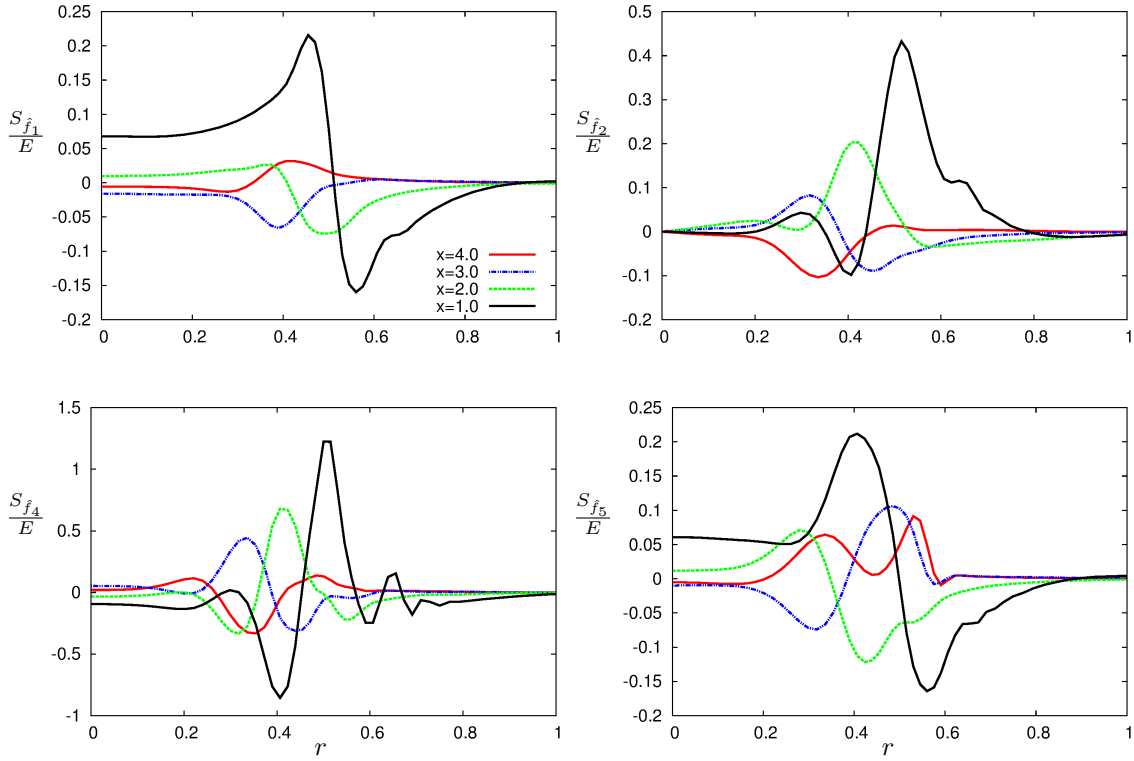


Figure 8. From top the bottom we have respectively, the sensitivity S_f computed for the underexpanded supersonic single jet with respect to the forcing acting in the continuity, r -momentum, x -momentum and energy equation at different fixed position in the stream-wise direction ($x = 4.0, 2.0, 1.0, 0.5$).

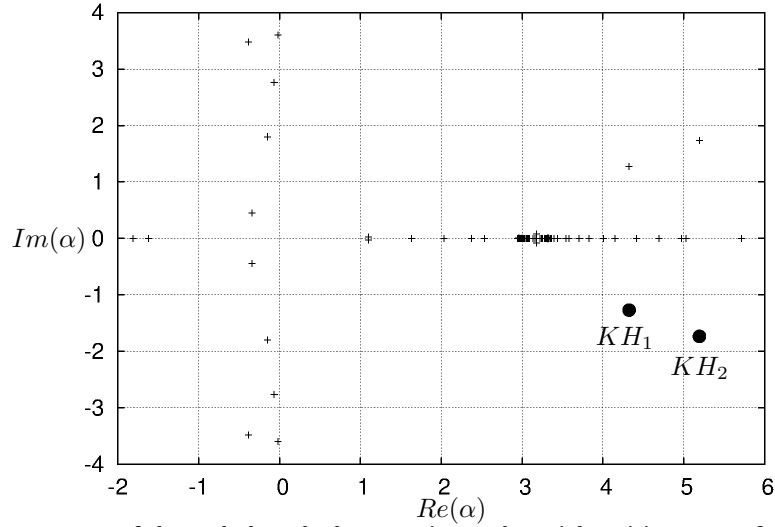


Figure 9. Stability spectrum of the turbulent dual-stream jet at the axial position $x = x_0$ for Strouhal number $St = 1.0$ and for azimuthal wavenumber $m = 0$. In full circle the 2 unstable modes related to Kelvin-Helmholtz instability in the primary KH_1 and secondary KH_2 jet.

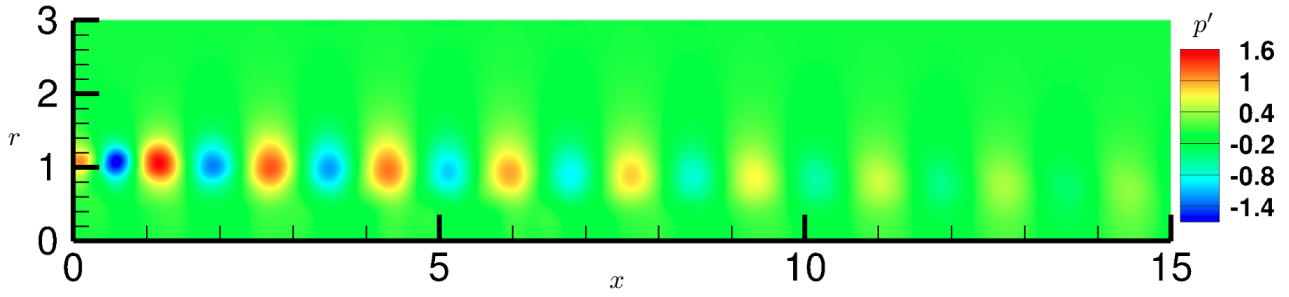


Figure 10. Spatial distribution of the perturbation p' for the Strouhal number $St = 1.0$ for the turbulent dual-stram jet initialized with the unstable mode KH_2 , the pressure growth in the secondary shear layer jet and fall-down for high values of the streamwise coordinates where the flow becomes stable.

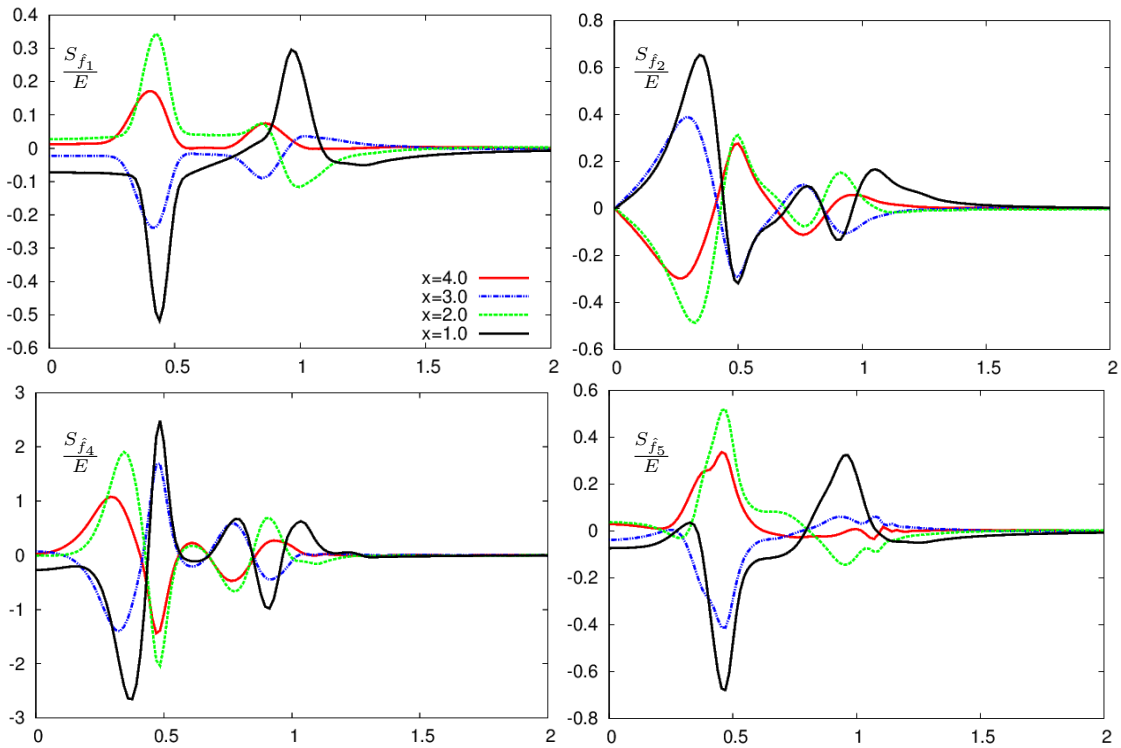


Figure 11. The results refer to the turbulent dual-stream jet initialized with the unstable mode KH_1 . From top the bottom we have respectively, the sensitivity S_f computed for the underexpanded supersonic dual-stream jet with respect to the forcing acting in the continuity, r -momentum, x -momentum and energy equation at different fixed position in the stream-wise direction ($x = 4.0, 2.0, 1.0, 0.5$).

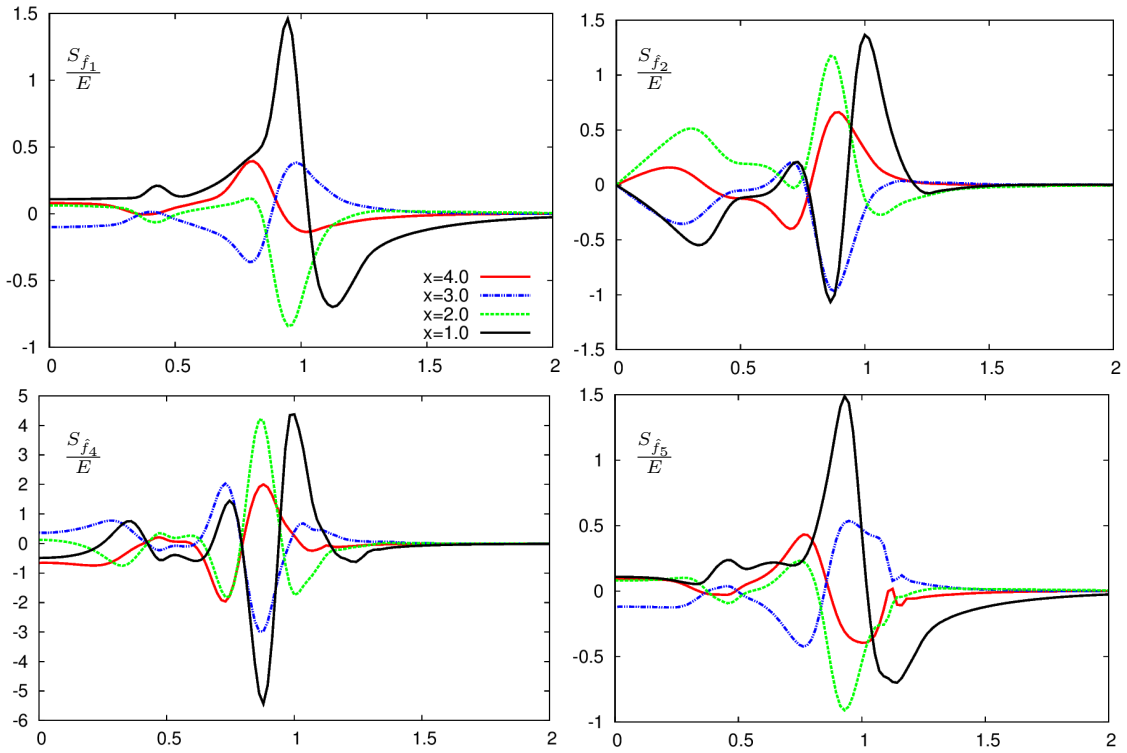


Figure 12. The results refer to the turbulent dual-stream jet initialized with the unstable mode KH_2 . From top the bottom we have respectively, the sensitivity S_f computed for the underexpanded supersonic dual-stream jet with respect to the forcing acting in the continuity, r -momentum, x -momentum and energy equation at different fixed position in the stream-wise direction ($x = 4.0, 2.0, 1.0, 0.5$).